Chemical Control of Electrical Properties and Phase Diagram of a Series of λ-Type BETS Superconductors, λ-$(BETS)_2GaBr_xCl_{4-x}$

Hisashi Tanaka,[†] Akiko Kobayashi,*[,†] Akane Sato,[‡] Hiroki Akutsu,[‡] and Hayao Kobayashi[‡]

Contribution from the Department of Chemistry, School of Science, The University of Tokyo, Hongo, Bunkyo-ku, Tokyo, 113-0033 Japan, and the Institute for Molecular Science, Myodaiji-cho, Okazaki, 444-8585 Japan

Received August 4, 1998

Abstract: λ-$(BETS)_2GaBr_xCl_{4-x}$ [BETS = bis(ethylenedithio)tetraselenafulvalene; $0 \le x \le 2$] is a molecular superconductor with strongly correlated conduction electrons. The electrical transport properties of λ-$(BETS)_2GaBr_x$-Cl_{4-x} are drastically changed by varying the bromine content x or by applying pressure. At ambient pressure, the superconducting transition could be observed for $x < 0.75$. The pressure and x dependencies of T_c were examined. The $M-H$ curve (M = magnetization; H = magnetic field) at 2 K indicated the almost perfect Meissner state of the superconducting phase of λ-$(BETS)_2GaCl_4$. The H_{c1} is ∼8 Oe for $H_\perp$ and 12 Oe for $H_{||}$, where $H_\perp$ and $H_{||}$ are the magnetic fields perpendicular and parallel to the c axis, respectively. The magnetic susceptibility of λ-$(BETS)_2GaBr_xCl_{4-x}$ increases with decreasing temperature to ∼60 K, below which the susceptibility becomes x-dependent and tends to be suppressed with increasing x. The isotropic decrease of the static susceptibility at lower temperature observed in the insulating system with $x > 1.0$ indicates the insulating ground state seems not to be antiferromagnetic but probably nonmagnetic. The crystal structure determinations of a series of λ-$(BETS)_2GaBr_xCl_{4-x}$ and the calculations of the intermolecular overlap integrals of the highest occupied molecular orbital of BETS were made to elucidate a key factor of the superconducting transition mechanism. The x-dependence of intermolecular overlap integrals seems to suggest that the magnitude of the "spin gap" of the nonmagnetic insulating state tends to be diminished with decreasing x. There exists one intermolecular overlap integral exhibiting a large temperature and x-dependence, which seems to play a crucial role in determining the nature of the ground state.

Introduction

Among the itinerant electron systems, molecular conductors and superconductors have occupied an important position, because of their unique physical properties that originate from the low-dimensional and narrow electronic band structures. Since the discovery of the first organic superconductor $(TMTSF)_2PF_6$ (TMTSF = tetramethyltetraselenafulvalene),[1] a number of molecular superconductors have been developed using planar π molecules such as TMTSF, bis(ethylenedithio)-tetrathiafulvalene (BEDT-TTF),[2] and $M(dmit)_2$ (M = Ni, Pd; dmit = 1,3-dithiol-2-thione-4,5-dithiolate).[3] Bechgaard salts $(TMTSF)_2X$ (X = PF_6, ClO_4, ...) and κ-type BEDT-TTF complexes are two types of representative organic superconducting systems whose physical properties and phase diagrams have been intensively studied. It is well-known that $(TMTSF)_2X$ is a one-dimensional conductor with a planelike Fermi surface whereas the κ-type ET conductor is a two-dimensional conductor with a cylindrical Fermi surface. Despite the difference in the dimensionality of their electronic structures, the phase diagrams of these two typical organic superconductors share common features. That is, the superconducting (SC) phase neighbors on the antiferromagnetic (AF) insulating phase. Needless to say, the AF insulating phase of $(TMTSF)_2X$ is the spin density wave (SDW) phase produced by the nesting of Fermi surfaces. The SDW state tends to transform into the SC state by applying pressure. In the famous Jerome's generalized temperature−pressure phase diagram,[4] $(TMTTF)_2X$ (TMTTF = tetramethyltetrathiafulvalene) is located at the lower pressure side of $(TMTSF)_2X$, where TMTTF is the sulfur analogue of TMTSF. Due to the small bandwidth and the large electron correlation, $(TMTTF)_2PF_6$ has a nonmagnetic spin-Peierls ground state, where localized spins tend to form spin-singlet pairs coupled with a periodical lattice distortion: ΔE (the difference between the first and second oxidation potentials), which is a rough measure of the on-site Coulomb interaction, is 0.34−0.35 V for TMTSF and 0.45 V for TMTTF.[5] The paramagnetic susceptibility decreases to zero isotropically at low temperature. The spin-Peierls ground state can be changed to the SDW state by applying pressure. Therefore, in the series of $(TMTCF)_2X$ (C = T or S), the ground state is believed to change with increasing pressure as spin-Peierls → SDW → SC. Unlike the SDW state of $(TMTSF)_2X$, the AF insulating state of κ-ET_2-$Cu[N(CN)_2]Cl$, which retains the highest T_c record since 1990

[†] The University of Tokyo.

[‡] Institute for Molecular Science.

(1) Jerome, D.; Mazaud, A.; Ribault, M.; Bechgaard, K. *J. Phys. Lett.* **1980**, *41*, L95−L98.

(2) Williams, J. M.; Ferraro, J. R.; Thorn, R. J.; Carlson, K. D.; Geiser, U.; Wang, H. H.; Kini, A. M.; Whangbo, M.-H. *Organic Superconductors*; Prentice Hall: Englewood Cliffs, NJ, 1992.

(3) Cassoux, P.; Valade, L.; Kobayashi, H.; Kobayashi, A.; Clark, R. A.; Underhill, A. E. *Coord. Chem. Rev.* **1991**, *110*, 115−160. Kobayashi, A.; Kim, H.; Sasaki, Y.; Moriyama, S.; Nishio, Y.; Kajita, K.; Sasaki, W.; Kato, R.; Kobayashi, H. *Synth. Met.* **1988**, *27*, B339−B346.

(4) Jerome, D. *Science* **1991**, *252*, 1509−1514.

(5) Papavassiliou, G. C.; Terzis, A.; Delhaes, P. In *Organic Conductive Molecules and Polymers*; Nalwa, H. S., Ed.; John Wiley & Sons: Chichester, 1997; p 173. Ogura, F.; Otsubo, T. In *Organic Conductive Molecules and Polymers*; Nalwa, H. S., Ed.; John Wiley & Sons: Chichester, 1997; p 234.

10.1021/ja9827806 CCC: $18.00
Published on Web 01/16/1999

(T_c = 12.8 K at 0.3 kbar),[6] originates from the strong correlation of two-dimensional conduction electron systems. It has been suggested that, in the insulating state, π electrons tend to localize on ET dimers to develop the AF spin structure.[7] By applying a very low pressure, the AF insulating state is converted into the SC state. Thus, despite the difference in the origins of the AF spin structures, the phase diagrams of the Bechgaard salts and κ-type ET superconductors seem to suggest an important role of the spin excitation in the SC transition mechanism in organic conductors. It should be recalled that nonphonon-mediated organic superconductivity was suggested by Fukuyama and Hasegawa in 1987 in the theoretical analysis[8] of the results of the NMR relaxation time of Bechgaard salts.[9]

However, we have recently reported a series of organic conductors based on bis(ethylenedithio)tetraselenafulvalene) (BETS) molecules, where a nonmagnetic insulating phase seems to be located near the SC phase. λ-$(BETS)_2GaCl_4$ [10,11] and λ-$(BETS)_2FeCl_4$[10] are two typical λ-type BETS conductors. Unlike λ-$(BETS)_2GaCl_4$ exhibiting a SC transition, the isostructural conductor containing magnetic anions, λ-$(BETS)_2FeCl_4$ undergoes a coupled metal−insulator (MI) and AF transition. Despite the large difference in the nature of the ground state, these two systems show very similar resistivity behaviors above 10 K. The round resistivity maximum around 90 K suggests the highly correlated state of π conduction electrons. Fortunately, it is not difficult to exchange not only central metal atoms (Ga, Fe) but also halogen atoms in tetrahedral anions without serious change of the crystal structure, which produces an extremely large variety of electronic properties such as the SC state of λ-$(BETS)_2GaBr_xCl_{4-x}$,[12] the colossal magnetoresistance of λ-$(BETS)_2FeCl_4$,[13] the coupled and decoupled MI and AF transitions of λ-$(BETS)_2FeBr_xCl_{4-x}$,[14] and a superconductor-to-insulator transition in λ-$(BETS)_2Fe_xGa_{1-x}Cl_4$.[15] We have never encountered such a fertile organic conducting system. As for the superconductivity, we have recently found that λ-$(BETS)_2GaBr_{1.5}Cl_{2.5}$ becomes a superconductor at high pressure, whose transition temperature (T_c = 9.7 K at 3 kbar) is almost the same as the revised precise T_c of the first so-called 10 K-class organic superconductor κ-$(BEDT\text{-}TTF)_2Cu(NCS)_2$.[16,17] Thus, the λ-type BETS superconductor can be regarded as a kind of 10 K-class organic superconductor. Furthermore, λ-$(BETS)_2GaBr_{1.5}Cl_{2.5}$ seems to take a nonmagnetic insulating state at ambient pressure. If the nonmagnetic insulating state really neighbors on the SC phase, the spin fluctuation cannot play a crucial role in the SC transition in λ-type BETS superconductors. Therefore, it is very important to clarify the low-temperature properties of λ-$(BETS)_2GaBr_xCl_{4-x}$. It is a very advantageous point in λ-type BETS superconductors that the electrical properties can be continuously controlled by changing the x-value of the tetrahalogenogallate anion, $GaBr_xCl_{4-x}^-$. In this paper, the crystal and electronic band structures, electrical and magnetic properties, and phase diagram of λ-$(BETS)_2GaBr_xCl_{4-x}$ are reported.

Experimental Section

Synthesis. All the chemical procedures were performed under an inert atmosphere. The solvents were reagent grade and freshly distilled. BETS was prepared according to the literature methods[18] and recrystallized from dichloromethane. λ-$(BETS)_2GaBr_xCl_{4-x}$ crystals were grown as needle crystals by electrochemical oxidation from the mixed solvent of 90% chlorobenzene and 10% ethanol containing BETS and tetraethylammonium tetrahalogenogallate. The constant current of 0.5 μA was applied for 10−15 days. H-shaped glass cells were used. We have recently reported the synthetic procedures using tetraethylammonium mixed halogenogallate $(Et_4N)GaX_xCl_{4-x}$ (X = Br, F).[12] However, in this work, except for the case of λ-$(BETS)_2GaCl_{3.0}F_{1.0}$, we adopted the mixed electrolytes of $(Et_4N)GaBr_4$ and $(Et_4N)GaCl_4$ instead of $(Et_4N)GaBr_xCl_{4-x}$, because the bromine content of the crystal (x) was found to be satisfactorily controlled by this method. In the solution containing x mol of $GaBr_4^-$ and 4 - x mol of $GaCl_4^-$, anions immediately exchanged their halogen atoms with each other and reached an equilibrium state where the NMR spectra showed the existence of $GaBr_4^-$, $GaBr_3Cl^-$, $GaBr_2Cl_2^-$, $GaBrCl_3^-$, and $GaCl_4^-$ anions. Therefore, $GaBr_xCl_{4-x}^-$ must be regarded as the average stoichiometry of these five tetrahalogenogallate ions.[19] In the present electrocrystallization experiments, the electrochemical oxidation was started after allowing the mixed electrolyte solution to stand for 24 h.

The x value was estimated by electron probe microanalysis (EPMA) and X-ray diffraction experiments. The crystals of λ-$(BETS)_2GaBr_xCl_{4-x}$ were obtained in the range of x values of $0 < x < 2.0$. But the λ-type crystals were not the main product for $x > 1.5$. When x was over 2.0, the crystals of another modification, λ′-$(BETS)_2GaBr_xCl_{4-x}$, were obtained.

Crystal Structure Determination. The X-ray data were obtained using a four-circle diffractometer (Rigaku AFC-7R) at room temperature and by a low-temperature Weissenberg-type imaging plate system (Mac Science DIP-320) at 7 K. Monochromated Mo Kα radiation (λ = 0.7107 Å) was used in all the X-ray experiments. The structure was solved by direct methods.[20] As for the room-temperature data, all the non-hydrogen atoms were anisotropically refined and the hydrogen atoms isotropically refined, while at low temperature, the carbon and hydrogen atoms were isotropically refined and the other atoms anisotropically refined. The occupancy probabilities of the halogen atoms were also refined.[21]

Electronic Band Structure Calculation. The electronic band structures of a series of λ-type BETS salts were calculated by using

(6) Williams, J. M.; Kini, A. M.; Wang, H. H.; Carlson, K. D.; Geiser, U.; Montgomery, L. K.; Pyrka, G. J.; Watkins, D. M.; Kommers, J. M.; Boryschuk, S. J.; Crouch, A. V. S.; Kwok, W. K.; Schirber, J. E.; Overmyer, D. L.; Jung, D.; Whangbo, M.-H. *Inorg. Chem.* **1990**, *29*, 3272−3274.

(7) Miyagawa, K.; Kawamoto, A.; Nakazawa, Y. Kanoda, K. *Phys. Rev. Lett.* **1995**, *75*, 1174−1177. Kawamoto, A.; Miyagawa, K.; Nakazawa, Y.; Kanoda, K. *Phys. Rev. Lett.* **1995**, *75*, 3455−3458.

(8) Hasegawa, Y.; Fukuyama, H. *J. Phys. Soc. Jpn.* **1987**, *56*, 877−880.

(9) Takigawa, M.; Yasuoka, H.; Saito, G. *J. Phys. Soc. Jpn.* **1987**, *56*, 873−876.

(10) (a) Kobayashi, H.; Udagawa, T.; Tomita, H.; Bun, K.; Naito, T.; Kobayashi, A. *Chem. Lett.* **1993**, 1559−1562. (b) Kobayashi, A.; Udagawa, T.; Tomita, H.; Naito, T.; Kobayashi, H. *Chem. Lett.* **1993**, 2179−2182.

(11) Montgomery, L. K.; Burgin, T.; Huffman, J. C.; Ren, J.; Whangbo, M.-H. *Physica* **1994**, *C219*, 490−496. Montgomery, L. K.; Burgin, T.; Miebach, T.; Dunham, D.; Huffman, J. C.; Schirber, J. E. *Mol. Cryst. Liq. Cryst.* **1996**, *284*, 73−84.

(12) Kobayashi, H.; Tomita, H.; Naito, T.; Tanaka, H.; Kobayashi, A.; Saito, T. *J. Chem. Soc., Chem. Commun.* **1995**, 1225−1226. Tanaka, H.; Kobayashi, A.; Saito, T.; Kawano, K.; Naito, T.; Kobayashi, H. *Adv. Mater.* **1996**, *8*, 812−815.

(13) Goze, F.; Laukhin, V. N.; Brossard, L.; Audouard, A.; Ulmet, J. P.; Askenazy, S.; Naito, T.; Kobayashi, H.; Kobayashi, A.; Tokumoto, M.; Cassoux, P. *Physica* **1995**, *B211*, 290−292. Brossard, L.; Clerac, R.; Tokumoto, M.; Ziman, T.; Petrov, D. K.; Laukhin, V. N.; Naughton, M. J.; Audouard, A.; Goze, F.; Kobayashi, A.; Kobayashi, H.; Cassoux, P. *Eur. Phys. J.* **1998**, *B1*, 439−452.

(14) Akutsu, H.; Arai, E.; Kobayashi, H.; Tanaka, H.; Kobayashi, A.; Cassoux, P. *J. Am. Chem. Soc.* **1997**, *119*, 12681−12682.

(15) Kobayashi, H.; Sato, A.; Arai, E.; Akutsu, H.; Kobayashi, A.; Cassoux, P. *J. Am. Chem. Soc.* **1997**, *119*, 12392−12393.

(16) Geiser, U.; Williams, J. M.; Carlson, K. D.; Kini, A. M.; Wang, H. H.; Klemm, R. A.; Ferraro, J. R.; Kumar, S. K.; Lykke, K. R.; Wurz, P.; Parker, D. H.; Fleshler, S.; Dudek, J. D.; Eastman, N. L.; Mobley, P. B.; Seaman, J. M.; Sutin, J. D. B.; Yaconi, G. A.; Stout, P. *Synth. Met.* **1993**, *56*, 2314−2322.

(17) Urayama, H.; Yamochi, H.; Saito, G.; Nozawa, K.; Sugano, T.; Kinoshita, M.; Sato, S.; Oshima, K.; Kawamoto, A.; Tanaka, J. *Chem. Lett.* **1988**, 55−58.

(18) Kato, R.; Kobayashi, H.; Kobayashi, A. *Synth. Met.* **1991**, *41−43*, 2093−2096.

(19) McGarvey, B. R. M.; Taylor, J.; Tuck,D. G. *Inorg. Chem.* **1981**, *20*, 2010−2013.

(20) teXsan: Crystal Structure Analysis Package, Molecular Structure Corp., The Woodlands, TX, 1985, 1992.

Table 1. Crystal Data of λ-BETS Salts with Mixed Halogenogallate Anions at Room Temperature (293 K)

	$GaCl_3F$	$GaBr_xCl_{4-x}$						
x [a]		0.00	0.31	0.50	0.70	1.29	1.50	2.00
x_{rg} [b]		—	0.35	0.48	0.71	1.22	1.49	1.90
a (Å)	16.167(6)	16.172(3)	16.204(3)	16.216(3)	16.238(3)	16.292(3)	16.320(3)	16.347(3)
b (Å)	18.605(5)	18.616(2)	18.614(2)	18.620(2)	18.625(4)	18.639(4)	18.650(4)	18.661(4)
c (Å)	6.608(1)	6.607(2)	6.6087(6)	6.610(1)	6.6105(10)	6.612(2)	6.614(1)	6.621(1)
α (°)	98.31(2)	98.38(2)	98.36(1)	98.36(1)	98.35(1)	98.35(2)	98.37(2)	98.40(2)
β (°)	96.82(2)	96.75(3)	96.70(1)	96.70(2)	96.67(2)	96.61(2)	96.54(2)	96.53(2)
γ (°)	112.59(2)	112.56(2)	112.52(1)	112.514(10)	112.489(10)	112.47(1)	112.46(1)	112.44(1)
V (Å^3)	1782.4(10)	1784.2(8)	1789.1(5)	1791.2(6)	1795.1(7)	1803.5(8)	1808(1)	1814.8(7)
R, Rw	0.046, 0.037	0.038, 0.030	0.037, 0.026	0.036, 0.021	0.058, 0.040	0.031, 0.019	0.057, 0.037	0.044, 0.028
Space group	$P\bar{1}$	$P\bar{1}$	$P\bar{1}$	$P\bar{1}$	$P\bar{1}$	$P\bar{1}$	$P\bar{1}$	$P\bar{1}$
No. of obs. ($I > 3.00\sigma(I)$)	3528	3611	3942	3714	3690	4963	2205	3578
No. of parameters	374	370	374	374	374	374	374	374
T_c (mid point /K)	3.5	6.0	6.5	7.0	7.3	8.0(1.3kbar)	9.7(3.0kbar)	— [c]

[a] x is calculated from the weight of electrolyte on preparation. [b] x_{rg} is a regression value calculated by the equation, $V = 1783.2 + 16.652x$, which is obtained by the least-squares method of V and x. [c] High-pressure resistivity could not be measured because of the fragileness of samples.

the extended Hückel tight-binding approximation on the basis of the highest occupied molecular orbitals (HOMOs) of BETS. In the calculation of overlap integrals, the difficult problem of the contribution from the d-orbitals of the chalcogen atoms is always encountered. Despite the many discussions about the Se-containing organic conductors such as TMTSF compounds,[22,23] this problem has not been settled. In the present calculation, we adopted the parameters without d-orbitals, because the d-orbitals gave anomalously large transverse intermolecular interactions.[24] However, in either case, with or without d-orbitals, the apparently similar two-dimensional Fermi surfaces were obtained.

Physical Properties. The electrical resistivities were measured along the thin needle axes of crystals (l||c) by the conventional four-probe method from room temperature to 1.5 K. Gold wires (0.015 mm diameter) were bonded to the crystals with conducting gold paste. The electrical resistivity under high pressure was measured by a clamp-type high-pressure cell. Silicone oil (Idemitsu Daphne No. 7373) was used as the pressure medium.

The magnetic susceptibility measurements were performed on a SQUID (Quantum Design MPMS-7, MPMS-5S, and MPMS-2) from 300 to 2 K using polycrystalline samples. The anisotropy of magnetization was measured using oriented thin needle crystals placed in quartz capillaries.

Results and Discussion

Crystal Structure and Bromine Content. The crystals of λ-$(BETS)_2GaBr_xCl_{4-x}$ are triclinic, with the space group $P\bar{1}$. The cell parameters at room temperature (293 K) are listed in Table 1, and those at 7 K are in Table 2. In Table 1, x was calculated from the mole ratio of $(Et_4N)GaBr_4$ and $(Et_4N)GaCl_4$ in the solution on the electrochemical oxidation. The correlation between the bromine content x and the unit cell volume V is well fitted by the linear relation, $V = 1783.2 + 16.652x$. By using this relation, we could estimate the bromine content x from the unit cell volume, which is in good agreement with the x-value determined by EPMA.[25] The lattice constant a increases fairly rapidly with increasing x, but the change is rather small in b and c. (Figure 1). The crystal structures of more than 10 crystals ($0.0 < x < 2.0$) were determined at room temperature. Table 1 shows the lattice constants of eight crystals. The crystal structures at 7 K were also determined for two crystals: one was a superconductor ($x = 0.31$) and the other was a semiconductor ($x = 1.29$) at ambient pressure. Neither a structural transition nor a remarkable change in the molecular structure was detected by changing the bromine content or temperature.

Table 2. Crystal Data of λ-$(BETS)_2GaBr_xCl_{4-x}$ Salts with Mixed Halogenogallate Anions at 7 K

	x	
	0.31	1.29
a (Å)	15.909(4)	15.996(11)
b (Å)	18.437(5)	18.421(10)
c (Å)	6.536(2)	6.535(5)
α (deg)	98.67(2)	98.78(5)
β (deg)	95.69(2)	95.50(7)
γ (deg)	111.97(2)	112.10(4)
V (Å^3)	1732(1)	1738(2)
R, R_w	0.066, 0.077	0.061, 0.083
no. of obs refctns ($I < 3.00\sigma(I)$)	4636	5199
no. of param	374	374
space group	$P\bar{1}$	$P\bar{1}$

The crystal structure of λ-$(BETS)_2GaBr_xCl_{4-x}$ at room temperature is shown in Figure 2. There are two crystallographically

(21) The occupancy probabilities of halogen atoms were refined as chlorine, and the bromine content on the site is estimated by this equation: (bromine content on the site) = 17(occupancy probability calculated as chlorine − 1)/(35 − 17).

(22) Grant, P. M. *Phys. Rev.* **1982**, *B26*, 6888−6895.

(23) Whangbo, M.-H.; Walsh, W. M., Jr.; Haddon, R. C.; Wudl, F. *Solid State Commun.* **1982**, *43*, 637−639.

(24) The ζ exponent (ionization potential (eV)) parameters for band calculation are as follows. Se: 4s 2.440 (−19.57), 4p 2.072 (−8.96). S: 3s 2.122 (−22.03), 3p 1.827 (−10.47). C: 2s 1.625 (−20.90), 2p 1.625 (−11.40). H: 1s 1.0 (−13.6).

(25) The results of elemental analysis by EPMA: $x = 0.00$, Ga:Br:Cl = 1.00:−:3.88. $x = 0.31$, Ga:Br:Cl = 1.00:0.31:3.80. $x = 0.50$, Ga:Br:Cl = 1.00:0.55:3.33. $x = 0.70$, Ga:Br:Cl = 1.00:0.65:3.26. $x = 1.29$, Ga:Br:Cl = 1.00:1.35:2.73. $x = 1.50$, Ga:Br:Cl = 1.00:1.56:2.36. $x = 2.00$, Ga:Br:Cl = 1.00:1.93:2.15. $GaCl_3F$, Ga:Cl = 1.00:3.09.

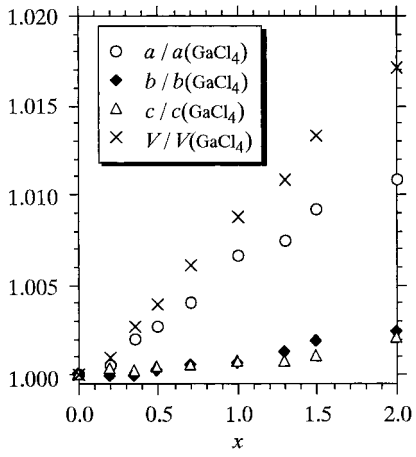

Figure 1. Bromine content (x) dependencies versus the lattice constants of λ-$(BETS)_2GaBr_xCl_{4-x}$ at room temperature. All data are normalized by the $x = 0.0$ (λ-$(BETS)_2GaCl_4$) value.

independent BETS molecules (I and II), which are stacked along the *a*-axis direction to form a 4-fold BETS column. The stacking pattern of BETS molecules can be expressed as [I−II*···II−I*]···[I−II*···II−I*], where the molecule with * indicates the molecule derived by the inversion symmetry. Anions are located on the open sites surrounded by terminal ethylene groups of BETS molecules (Figure 2a). There are two dimers (I−II* and II−I*) in one repeating unit. Three intermolecular overlap modes, A(I−II*), B(II*-II), and C(I−I*), are shown in Figure 2c. In mode A, two BETS molecules overlap each other, sliding along the long axis of the molecule by ∼1.2 Å. In mode B, the sliding distance along the long axis of the molecule is ∼3.0 Å. The molecules are also slipped to the transverse direction (0.5 Å) to avoid any direct contact of the neighboring chalcogen atoms. The interplanar distances between the BETS molecules becomes very large as will be described below. In mode C, the sliding distance is over 4.5 Å. When the bromine content increases from $x = 0.0$ to 2.00, the interplanar distances between BETS molecules change as follows: (A) 3.769 → 3.788 Å (0.5% increase), (B) 4.037 → 4.054 Å (0.4% increase), and (C) 3.847 → 3.885 Å (1.0% increase). The increase in the interplanar distance in mode C is about twice the others, which shows the sensitivity of the intermolecular interaction C versus the *x*-values.

As mentioned in the Experimental Section, there exist five kinds of tetrahalogenogallate anions, $GaBr_4^-$, $GaBr_3Cl^-$, $GaBr_2Cl_2^-$, $GaBrCl_3^-$, and $GaCl_4^-$, at chemical equilibrium in solution so that it is natural to consider that the anion sites are occupied by these five tetrahalogenogallate anions with the average stoichiometry of $GaBr_xCl_{4-x}^-$. Therefore, there are two types of anion disorders in the λ-type crystal. One is the disorder of these five species in the anion sites, or which species occupies the anion sites. The other is the orientational disorder of the anions, or which halogen site is better for the large bromine atoms to occupy among the four halogen sites of GaX_4^-. The disorder of the anion in the organic superconductor frequently produces serious effects on the electrical transport properties and T_c.[26] However, the effect of the disorders is found to be very small in the λ-type BETS salts.

The occupancies of bromine on the four halogen sites are listed in Table 3, which are estimated by the X-ray crystal structure refinements at room temperature (293 K) and at low temperature (7 K). The total bromine content was in good agreement with the bromine content in the solution from which the crystals were grown. Thus, λ-type BETS crystals with the desired bromine content could be prepared. However, the crystal quality became insufficient for $x > 1.5$.

The bromine distribution is not completely random but there are preferred positions (X2 and X4 (see Figure 2a)). The first line in Table 3 represents the occupancies of bromine on sites X1−X4, and the second line indicates the normalized probability (%), where the sum of the bromine occupancies over the four halogen sites is defined as 100%. The bromine occupancy is largest on site X2 and smallest on site X3 for every crystal (X2 > X4 > X1 > X3). With increasing bromine content, each bromine occupancy tends to be leveled off. On the contrary, the occupancies on X2 and X4 (X1 and X3) tend to be enhanced (decreased) at low temperature. This means a decrease in the orientational randomness of the nontetrahedral anions with decreased temperature. Roughly speaking, two-thirds of the bromine atoms are located on X2 and the remaining one-third are on X4 at low temperature and $x < 0.5$. It may be said that the change in the bromine distribution will affect the arrangement of the donor molecules and result in a change in the band structures, as will be described below.

Resistivities of λ-$(BETS)_2GaCl_4$ and λ-$(BETS)_2GaCl_{3.0}F_{1.0}$. The general features of the *x*-dependence of the resistivity behavior of λ-$(BETS)_2GaBr_xCl_{4-x}$ have been reported in a previous paper.[27] We will now report the more detailed electrical transport properties of the λ-type BETS conductors.

As shown in Figure 3, the temperature dependence of the resistivity of the λ-type BETS conductors shows a systematic variation according to the difference in the anion size (bromine content). We have interpreted the resistivity change in terms of the "chemical pressure effect".[12] The room-temperature resistivity of λ-$(BETS)_2GaCl_4$ is about 0.03 Ωcm. The resistivity shows a broad maximum around 90 K (Figure 3). The nonmetallic behavior above 90 K indicates a strong correlation of the π-electron system. The resistivity rapidly decreased below 90 K and showed a sharp drop around 6 K. Based on the observation of the SC transition in λ-$(BETS)_2GaCl_4$, we have frequently encountered the crystals which showed a gradual resistivity drop at fairly high temperature (the onset of temperature, $T_{on} \approx 8$ K).[28] It seemed that such a resistivity behavior will be due to the "effective (negative) pressure" produced at a small portion of the thin needle crystal by bonding four gold wires with gold paint. However, we have recently noticed that for the systematic comparison of the transition temperatures of a series of superconductors, λ-$(BETS)_2GaBr_xCl_{4-x}$, T_c must be taken as the middle point of the temperature where the resistivity sharply decreases from finite to zero. The determined T_c of λ-$(BETS)_2GaCl_4$ ($T_c \approx 6$ K) is about 2 K lower than that reported in the first paper.[10] The pressure dependence of the resistivity is given in Figure 4. The resistivity maximum around 90 K disappears above 2.4 kbar. With increasing pressure, T_c decreases almost linearly ($dT_c/dP = -0.72$ deg/kbar). At high pressure, the increase in the bandwidth will diminish the effect of the electron correlation and therefore the normal metallic resistivity behavior will be realized. A similar change can be expected when a smaller size anion is used because the decrease of the unit cell volume makes the intermolecular contacts of the BETS molecules more compact. In fact, the resistivity behavior of λ-$(BETS)_2GaCl_{3.0}F_{1.0}$ (Figure 3) at ambient pressure

(26) Tokumoto, M.; Anzai, H.; Murata, K.; Kajimura, K.; Ishiguro, T. *Synth. Met.* **1988**, *27*, A251−256.

(27) (a) Kobayashi, H.; Akutsu, H.; Arai, E.; Tanaka, H.; Kobayashi, A. *Phys. Rev.* **1997**, *B56*, R8526−8529. (b) Kobayashi, H.; Arai, E.; Naito, T.; Tanaka, H.; Kobayashi, A.; Saito, T. *Synth. Met.* **1997**, *85*, 1463−1464.

(28) Kobayashi, H.; Tomita, H.; Udagawa, T.; Naito, T.; Kobayashi, A. *Synth. Met.* **1995**, *70*, 867−870.

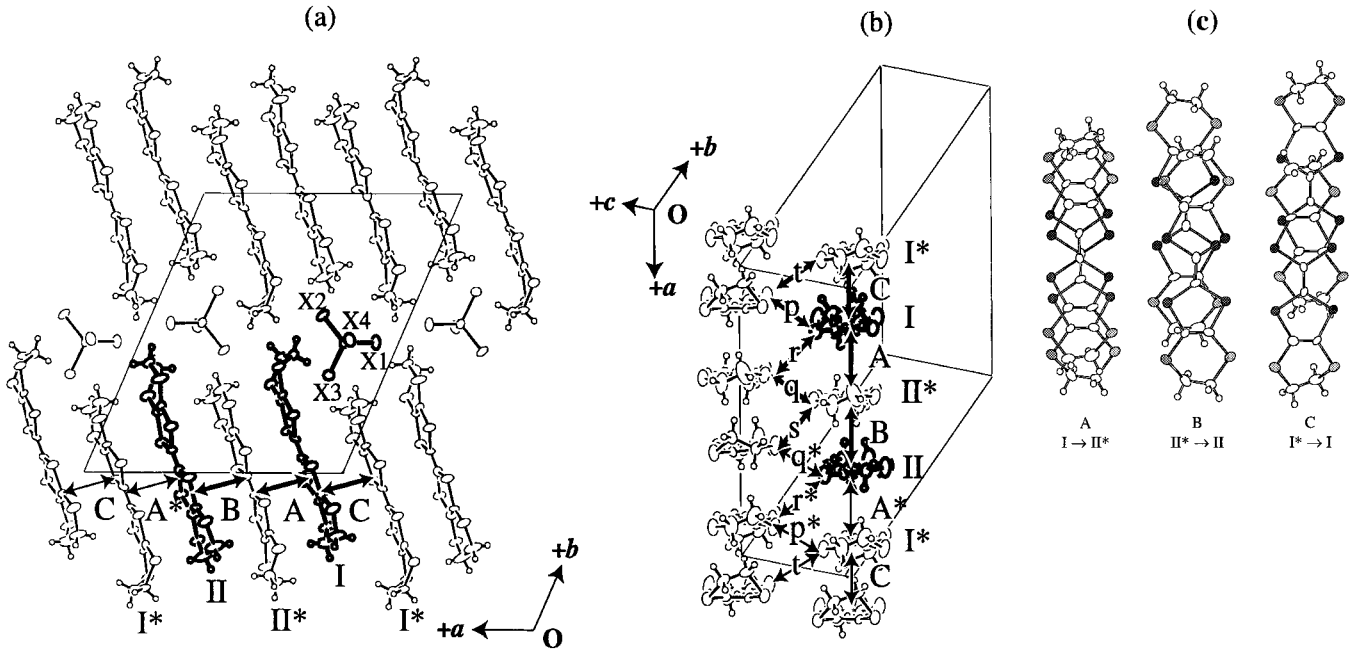

Figure 2. Crystal structure of λ-$(BETS)_2GaBr_xCl_{4-x}$ viewed along the *c*-axis (a), along the averaged long molecular axis (b), and modes of molecular overlap (c). (a, b) There are two crystallographically independent molecules I and II illustrated by the bold lines. The molecule with * indicates the molecule derived by the inversion symmetry. (c) The light- and dark-shaded atoms represent sulfur and selenium atoms, respectively.

Table 3. Occupancy of Bromine on Each Halogen Site of Anion of λ-$(BETS)_2GaBr_xCl_{4-x}$ at Room Temperature (293 K) and at Low Temperature (7 K)[a]

	halogen site (293 K)				
x	X1	X2	X3	X4	total
0.31	0.050(7) (16.4)	0.152(7) (49.8)	0.015(6) (5.0)	0.088(7) (28.8)	0.306(7)
0.50	0.086(5) (16.1)	0.249(4) (46.1)	0.042(5) (7.8)	0.161(4) (29.9)	0.539(5)
0.70	0.098(4) (14.8)	0.291(4) (43.8)	0.060(4) (9.1)	0.215(4) (32.4)	0.665(4)
1.29	0.215(4) (17.6)	0.503(3) (41.2)	0.138(4) (11.3)	0.366(4) (30.0)	1.223(4)
1.49	0.294(5) (18.4)	0.602(5) (37.7)	0.226(5) (14.2)	0.476(4) (29.8)	1.597(5)
2.00	0.352(7) (18.6)	0.699(7) (36.9)	0.270(7) (14.3)	0.574(7) (30.3)	1.896(7)
	halogen site (7 K)				
x	X1	X2	X3	X4	total
0.31	0.007(9) (2.3)	0.210(9) (62.3)	0.017(9) (5.0)	0.102(9) (30.4)	0.337(9)
1.29	0.165(10) (12.9)	0.592(9) (46.3)	0.313(9) (2.5)	0.490(9) (38.3)	1.279(9)

[a] First line of each set of data, bromine occupancy on the site. Second line, normalized bromine occupancy (%).

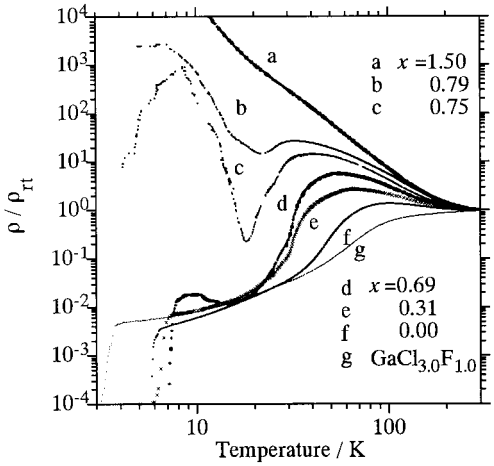

Figure 3. Temperature dependence of resistivity of λ-$(BETS)_2GaBr_xCl_{4-x}$. The resistivity drastically changes by varying the bromine content *x*. When $0.55 < x < 0.75$, the resistivity maximum below 15 K is observed. The resistivity of λ-$(BETS)_2GaCl_{3.0}F_{1.0}$ decreases monotonically without showing any resistivity maximum with lowering temperature. Each resistivity is normalized by the respective room-temperature resistivity.

closely resembles that of λ-$(BETS)_2GaCl_4$ at 2.4 kbar (see Figures 3 and 4). In λ-$(BETS)_2GaCl_{3.0}F_{1.0}$, the broad resistivity maximum around 90 K was not observed at ambient pressure and the T_c was 3.5 K.

Meissner Effect of λ-$(BETS)_2GaCl_4$. The anisotropy of the Meissner effect and the critical magnetic fields were measured on λ-$(BETS)_2GaCl_4$ over the magnetic field (*H*) range of 1−70 000 Oe using the oriented thin needle crystals. According to the measurement of diamagnetism, the SC state is almost in a perfect Meissner state. The Meissner volume was 115% when *H* was applied perpendicular to the *c*-axis ($H_{\perp c}$), while it was almost 30% for $H_{\parallel c}$; the magnetic susceptibility ($M/H = -1/4\pi$) corresponding to the full Meissner state is −50 emu/mol. The correction of the diamagnetic terms depending on the shape of the sample was not applied.

Figure 5 shows the $-M$ vs *H* curve at 2 K, which shows that λ-$(BETS)_2GaCl_4$ is a Type II superconductor. According to Figure 5, the lower critical magnetic fields (H_{c1}) were estimated as $H_{\parallel c,c1} \approx 12$ Oe and $H_{\perp c,c1} \approx 8$ Oe. However, $H_{\parallel c,c2}$ ($\sim 10^5$ Oe) and $H_{\perp c,c2}$ ($\sim 3 \times 10^4$ Oe) could not be precisely determined. It should be noted that the value perpendicular to the *c*-axis is the averaged value of all directions perpendicular to the *c*-axis and not exactly parallel to the *a*-axis or *b*-axis (conduction plane is the *ac* plane). Therefore, the lower and upper critical magnetic fields parallel to the *b*-axis might be much smaller. Considering the very sharp angular dependence of the magnetic field (10 000 Oe) effect on the superconductivity previously reported,[10a] H_{c2}

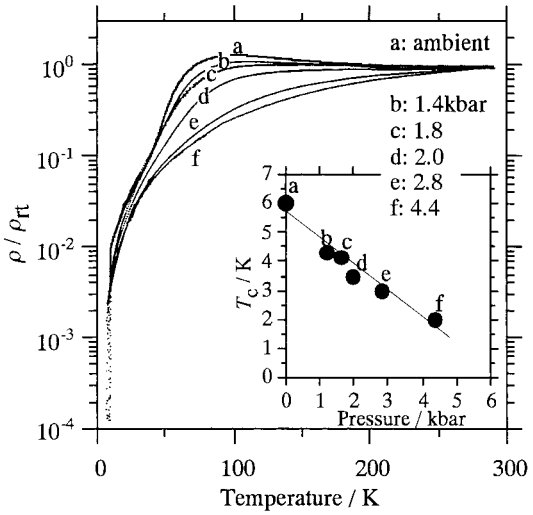

Figure 4. Pressure dependence of resistivity and T_c (midpoint) of λ-$(BETS)_2GaCl_4$ (inset).

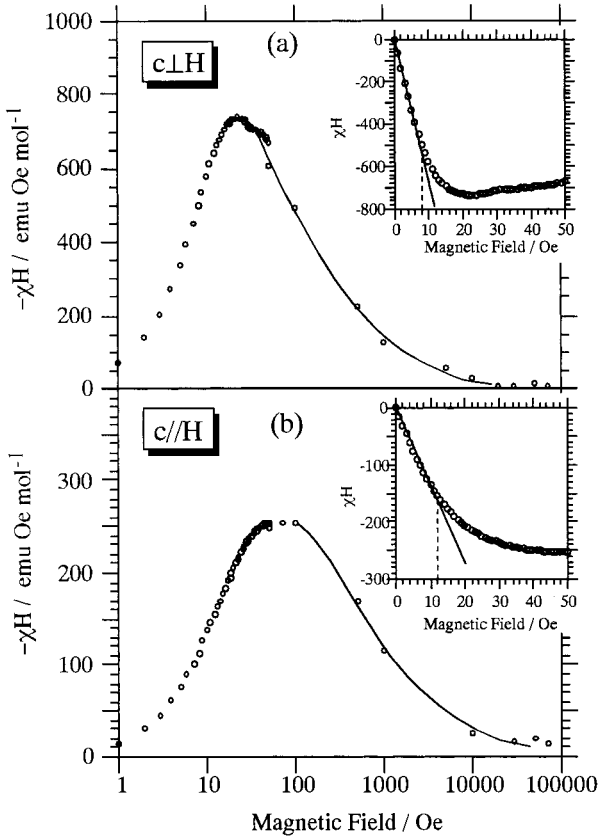

Figure 5. Field dependence of magnetization of λ-$(BETS)_2GaCl_4$ applying magnetic field perpendicular (a) and parallel (b) to the *c*-axis. The inset shows the magnetization of low applied field region.

will be less than 10 000 Oe for the field perpendicular to the conduction plane.

Resistivities of λ-$(BETS)_2GaBr_xCl_{4-x}$. The exchange of Cl in $GaCl_4$ to Br expands the unit cell volume and produces a "negative chemical pressure". With increasing Br content (*x*), the room-temperature resistivity increases from $\rho_{rt} = 0.03$ ($x = 0.00$) to 0.1 ($x = 2.00$) Ω cm and the broad resistivity maximum became prominent ($x < 0.75$, see Figure 4): $\rho_{max}/\rho_{rt} = 1.4$ ($x = 0.0$), 2.7 ($x = 0.31$), 5.8 ($x = 0.69$), 16 ($x = 0.75$), and 28 ($x = 0.79$). The temperature corresponding to the broad resistivity maximum decreased from 90 ($x = 0.0$) to 30 K ($x = 0.79$). In addition, another resistivity peak was observed below 15 K for

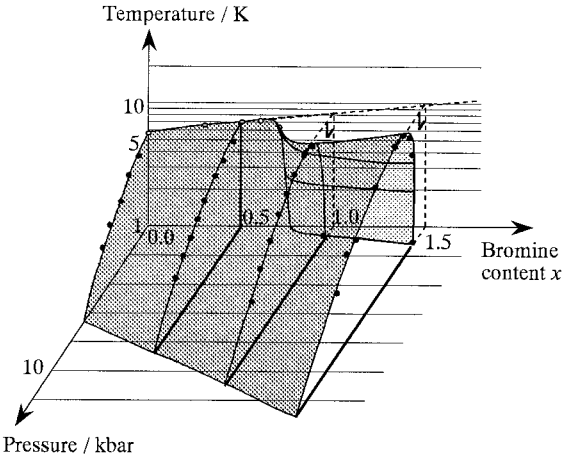

Figure 6. $T-P-x$ phase diagram of λ-$(BETS)_2GaBr_xCl_{4-x}$. The region surrounded by shaded plane corresponds to the superconducting region. When $x > 0.8$, the superconducting transition does not occur under ambient pressure.

$0.55 < x < 0.75$. After taking a sharp resistivity increase (ρ_{max}/ρ_{min} (~15 K) $< 5 \times 10^3$), the system undergoes a SC transition below 7.5 K. However, the SC transition was not clearly observed at $x > 0.75$. The enhancement of T_c with increasing *x* ($0.0 < x < 0.75$) is consistent with the effect of "negative pressure". At $x > 0.8$, the resistivity peak below 15 K and the broad resistivity maximum around 30 K were merged into one. The temperature dependence of resistivity then became non-metallic throughout the temperature range. However, as will be mentioned in next section, the magnetic properties change at low temperature, at least for $x > 1.0$. It has been reported that almost the same resistivity behavior can be realized by applying pressure to the semiconducting λ-$(BETS)_2GaBr_{1.5}Cl_{2.5}$.[27a] The maximum T_c of λ-$(BETS)_2GaBr_{1.5}Cl_{2.5}$ is 9.7 K at 3 kbar, which is higher than the maximum T_c (~7.5 K) observed in λ-$(BETS)_2GaBr_xCl_{4-x}$ ($x \approx 0.7$) at ambient pressure.

The Arrhenius fitting of the resistivity curves between 150 and 300 K gave the activation energy E_a as 5 ($x = 0.00$), 9 ($x = 0.35$), 16 ($x = 0.69$), and 24 meV ($x = 1.50$). The compound behaves as a semiconductor down to low temperature at $x > 0.80$, where the temperature dependence of the resistivity becomes stronger at low temperatures. This is consistent with the existence of the magnetic transition at low temperature (as will be described later).

The pressure dependence of T_c is very small ($dT_c/dP = -0.66$ deg/kbar) for $x = 0.5$, and the SC state seems to survive up to ~10 kbar. It is well-known that the pressure dependence of T_c for κ-type BEDT-TTF superconductors is much stronger: $dT_c/dP = -3.4$ (κ-$ET_2Cu[N(CN)_2]Cl$),[6] −1.3 (κ-$ET_2Cu(NCS)_2$),[17] and −0.8 deg/kbar (κ-ET_2I_3).[29]

Similar measurements were also made for the crystal with $x = 1.0$. Based on all the results of the high-pressure resistivity measurements ever made ($x = 0.0, 0.5, 1.0, 1.5$),[12,27] the $T-P-x$ phase diagram of λ-$(BETS)_2GaBr_xCl_{4-x}$ is drawn in Figure 6. The region surrounded by the shaded plane corresponds to the SC region. The maximum T_c (9.7 K) is obtained at $x = 1.5$ and 3 kbar, but at ambient pressure, the maximum T_c is 7.5 K. T_c tends to be enhanced with increasing *x*, suggesting the T_c around $x \approx 2.0$ will exceed 10 K. However, no further trial was made because of the insufficient crystal quality in the higher *x* region.

Magnetic Susceptibility and Phase Diagram. The resistivity behavior of the λ-type BETS conductor is considered to be

(29) Kobayashi, H.; Kawano, K.; Naito, T.; Kobayashi, A. *J. Mater. Chem.* **1995**, *5*, 1681−1687.

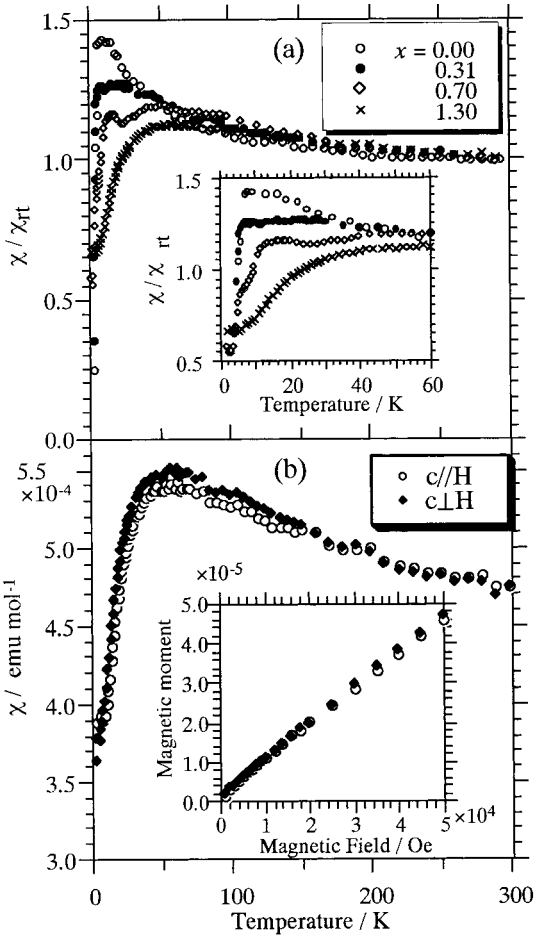

Figure 7. Magnetic susceptibilities of λ-(BETS)$_2$GaBr$_x$Cl$_{4-x}$. (a) Each susceptibility is normalized by the respective room-temperature susceptibility. (b) The magnetic susceptibility of λ-(BETS)$_2$GaBr$_{1.3}$Cl$_{2.7}$ perpendicular and parallel to the *c*-axis and inset shows field dependence of the magnetization measured at 5 K.

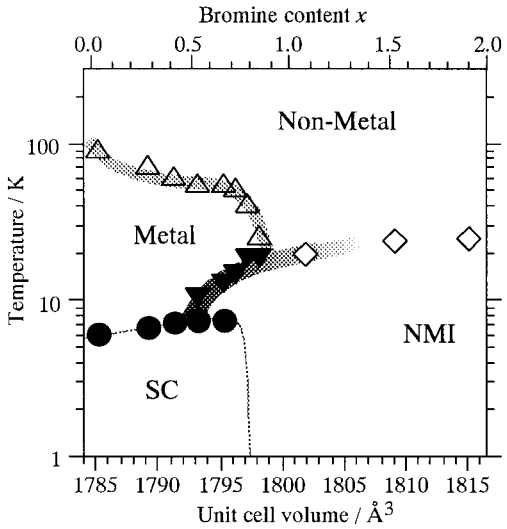

Figure 8. $T-x$ phase diagram of λ-(BETS)$_2$GaBr$_x$Cl$_{4-x}$ proposed by the result of resistivity and susceptibility. The upper (lower) abscissa represents bromine content x (unit cell volume). NMI, nonmagnetic insulating state.

related to the nature of the strongly correlated electron systems. The static susceptibilities of the polycrystalline samples of λ-(BETS)$_2$GaBr$_x$Cl$_{4-x}$ are shown in Figure 7a, where the core diamagnetisms were corrected. The applied field was 10 000 Oe for $x = 0.00$ and 0.31 and 5000 Oe for $x = 0.70$ and 1.30. The susceptibility at room temperature shows a slight dependence on x from $(4.5 \pm 0.2) \times 10^{-4}$ ($x = 0.0$) to $(4.9 \pm 0.2) \times 10^{-4}$ ($x = 1.30$) emu/mol. The susceptibility of every sample slowly increases with lowering the temperature at least to 60 K. The temperature dependence of the susceptibility shows a clear x-dependence below 60 K. At low temperature, the susceptibility tends to decrease with increasing x. At first, this behavior is not consistent with the expected enhancement of the electron correlation for the higher x-system, but the susceptibility behavior of the system with $x = 0.7$ is reminiscent of that for the κ-BEDT-TTF superconductor.[7] As will be mentioned later, one possible interpretation of this characteristic T- and x-dependencies of the susceptibility might be the effect of the antiferromagnetic fluctuation, which seems to be large in the system located near the boundary between the insulating phase and SC phase, that is, the system around $x \approx 0.7$.

In addition, the susceptibility of the system with $x = 0.70$ showed anomalies at 22 and 8 K, which roughly correspond to metal-to-insulator and insulator-to-SC transitions, respectively. When x is 1.30, the susceptibility showed a large decrease around 25 K. The anisotropy of the susceptibility of λ-(BETS)$_2$GaBr$_{1.3}$Cl$_{2.7}$ was examined using the oriented thin needle crystals. As seen from Figure 7b, the susceptibility was nonzero at 0 K, which seems to be ascribed not only to the incomplete subtraction of the Curie term of the impurities. No indication of the anisotropy could be observed. Furthermore, the measurement of the M−H curve at 5 K showed no trace of spin-flop-like behavior from 0 to 50 000 Oe at 5 K (inset of Figure 7b). Therefore, it seems that despite the nonzero susceptibility at 0 K, the ground state of λ-(BETS)$_2$GaBr$_x$Cl$_{4-x}$ ($x \approx 1.3$) is not simply antiferromagnetic but rather nonmagnetic. Essentially, the same susceptibility behavior was also observed for λ-(BETS)$_2$GaBr$_{1.0}$Cl$_{3.0}$ and λ-(BETS)$_2$GaBr$_{1.5}$Cl$_{2.5}$.[27a]

We have already reported the phase diagram of λ-(BETS)$_2$GaBr$_x$Cl$_{4-x}$,[27] but a revised phase diagram based on recent experimental results is presented in Figure 8. The unfilled triangles on the border between the nonmetal and metal phases represent a resistivity maximum around 50−100 K. At $x < 0.55$, the system showed a broad resistivity maximum and a metal−superconductor transition at low temperature. At $0.55 < x < 0.75$, the resistivity behavior changes as semiconductor → metal → insulator → superconductor. At $x > 0.8$ (volume >1798 Å^3), the system is nonmetallic and has an insulating ground state.

To obtain more magnetic information, ESR experiments were done but the ESR signal could not be obtained from room temperature to 4 K because of the broad line width due to the large spin−orbit coupling of selenium and the small signal intensity.

Electronic Band Structure. Although the 2:1 stoichiometry and the 4-fold stacking structure suggest the one-dimensional semiconducting properties of λ-type BETS conductors, they provide a series of superconductors. This is due to the two-dimensional electronic band structure.[11,30] Due to the dimeric arrangement of the BETS molecules, four HOMO bands are split into the upper two and lower two bands.

The dispersion relations of the HOMO bands and two-dimensional Fermi surface of λ-(BETS)$_2$GaBr$_x$Cl$_{4-x}$ ($x = 0.00$ and 2.00) calculated on the basis of the extended Hückel tight-binding band approximation are shown in Figure 9. The solid and dotted lines represent the calculations for $x = 0.00$ and $x = 2.00$, respectively. Needless to say, the Fermi surface of the

(30) Kobayashi, H.; Tomita, H.; Naito, T.; Kobayashi, A.; Sakai, F.; Watanabe, T.; Cassoux, P. *J. Am. Chem. Soc.* **1996**, *118*, 368−377.

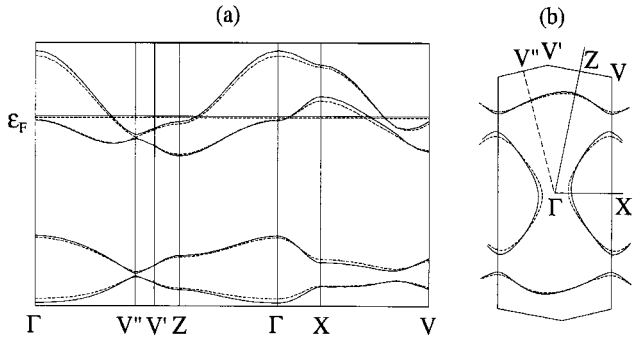

Figure 9. Dispersions of band structures (a) and Fermi surfaces of λ-$(BETS)_2GaBr_xCl_{4-x}$ at room temperature (b). The solid lines and dotted lines represent the calculations for $x = 0.00$ and 2.00, respectively.

Table 4. Overlap Integrals of λ-Type BETS Salts at Room Temperature (293 K) and at Low Temperature (7 K)[a]

		293 K				7 K	
	$x =$ 0.00	$x =$ 0.31	$x =$ 0.70	$x =$ 1.29	$x =$ 2.00	$x =$ 0.31	$x =$ 1.29
A	23.8	24.1	24.0	23.6	23.6	27.5	27.0
		(101)	(101)	(99)	(99)	(115)	(113)
B	9.84	9.87	9.66	9.54	9.62	11.3	11.4
		(100)	(98)	(97)	(98)	(115)	(116)
C	5.76	5.48	5.27	5.15	4.61	7.22	6.87
		(95)	(92)	(89)	(80)	(125)	(119)
p	−1.27	−1.29	−1.31	−1.29	−1.31	−1.66	−1.74
		(101)	(103)	(101)	(103)	(130)	(137)
q	−3.07	−3.08	−3.03	−3.17	−2.97	−3.68	−3.93
		(100)	(99)	(103)	(97)	(120)	(128)
r	3.69	3.54	3.49	3.48	3.42	3.64	3.94
		(96)	(95)	(94)	(93)	(99)	(107)
s	4.83	4.71	4.59	4.56	4.52	5.01	4.12
		(98)	(95)	(94)	(94)	(104)	(85)
t	0.408	0.392	0.377	0.325	0.313	0.324	0.273
		(96)	(92)	(80)	(77)	(79)	(67)

[a] First line of each set of data, overlap integrals ($\times 10^{-3}$). Second line, percentage against those of $x = 0.00$ at room temperature.

semiconducting λ-$(BETS)_2GaBr_{2.0}Cl_{2.0}$ system is artificial. The bandwidth of λ-$(BETS)_2GaCl_4$ is slightly larger than that of λ-$(BETS)_2GaBr_{2.0}Cl_{2.0}$.

The intermolecular overlap integrals (s) of the HOMOs of λ-$(BETS)_2GaBr_xCl_{4-x}$ ($x = 0.0$, 0.31, 0.70, 1.29, 2.00) calculated at room temperature are listed in Table 4. Symbols A−C and p−t are shown in Figure 2b. The interactions between the different conduction planes are negligible. The first line represents the overlap integrals, and the second line is the percentage versus those of $x = 0.00$. As was expected, the intradimer overlap integral s_A is much larger than the others. Due to the transverse ovelap integrals (s_q, s_r, s_s), slightly smaller than s_C, the upper two bands were merged into one and an effectively half-filled narrow band was produced. Thus, this simple tight-binding band structure will support the viewpoint that the system locates near the boundary between the Mott insulator and strongly correlated metal.

Figure 10a shows the x-dependence of the intermolecular overlap integrals at 293 K. The overlap integrals s_A, s_B, s_p, and s_q are almost independent of x, while s_C and s_t are strongly dependent on x. The overlap integrals s_r and s_s are intermediate. Neglecting s_t because of its very small value, it should be noted that only s_C exhibits a large x-dependence at $x > 0.7$. If we consider the one-dimensional electronic structure along the BETS stack, the constant s_A and s_B and the diminished s_C in the large-x region will imply an increase in the band gap, which

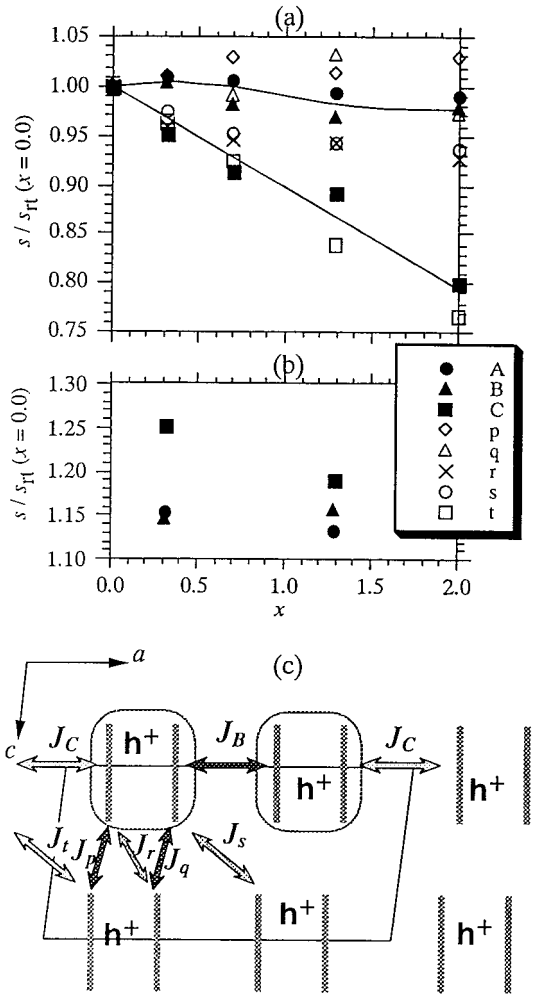

Figure 10. x-Dependence of intermolecular overlap integrals (s) at 293 K (a) and at 7 K (b) and schematic drawing of the insulator model of λ-$(BETS)_2GaBr_xCl_{4-x}$ viewed along the averaged long molecular axis (c). (a, b) Overlap integrals are normalized by each s of $x = 0.00$ at room temperature. Only overlap integrals' stacking direction of BETS is illustrated at 7 K. (c) The shaded bar and h^+ represent BETS molecule and hole existing in every BETS dimer. With increasing bromine content x, J_C and J_t are weakened, while J_B, J_p, and J_q are almost independent of x, which is represented by shading of arrows.

is consistent with the enhancement of the nonmetallic nature of λ-$(BETS)_2GaBr_xCl_{4-x}$ at higher x.

Table 4 shows the overlap integrals at 7 K. The first line represents the overlap integrals and the second line shows the percentage versus the room-temperature value. The changed percentage of the $x = 0.31$ system is almost identical to that of the $x = 1.29$ system; that is, s_A, s_B, s_C, s_p, and s_q are significantly increased. It is natural that most of the interactions become large at 7 K. It should be mentioned that the overlap integral s_C is much enhanced at low temperature, and furthermore, the enhancement of $x = 0.31$ is larger than that of $x = 1.29$ (Figure 10b). The increase in s_C at low temperature indicates the enhancement of the metallic nature of the system, which is consistent with the gradual semiconductor-to-metal transition around 30−90 K ($x < 0.75$).

Structural Aspect of the Phase Diagram. Recently, we reported the coupled and decoupled AF and MI transitions of λ-$(BETS)_2FeBr_xCl_{4-x}$.[14,31] We have also presented an AF spin structure model to explain the magnetization drop observed at

(31) Akutsu, H.; Kato, K.; Ojima, E.; Kobayashi, H.; Tanaka, H.; Kobayashi, A.; Cassoux, P. *Phys. Rev.* **1998**, *B58*, 9294−9302.

T_{MI} for λ-$(BETS)_2FeCl_4$.[13,14] As previously mentioned, the general feature of the resistivity behavior of λ-$(BETS)_2FeBr_xCl_{4-x}$ closely resembles that of λ-$(BETS)_2GaBr_xCl_{4-x}$ except for the low-temperature region. The round resistivity maximum observed around 50−90 K suggests that the system is located near the boundary between the Mott insulator and strongly correlated metal. Due to the strong correlation, the π conduction electrons tend to be localized on BETS dimers interrelated by interaction A (see Figure 2a and b). We have considered that the magnetization drop at T_{MI} in λ-$(BETS)_2FeCl_4$ can be regarded as evidence of the existence of the localized electron on each BETS dimer.[14] A similar situation can be expected in λ-$(BETS)_2GaBr_xCl_{4-x}$. However, it should be noted that the 4-fold structure will tend to produce the spin-Peierls-like state if π electrons are localized on the BETS dimers despite the fairly large transverse q, r, and s interactions (Table 4).

As already mentioned, the magnetic susceptibility measurements suggest that the insulating ground state of λ-$(BETS)_2GaBr_xCl_{4-x}$ is not simple AF but rather nonmagnetic. Therefore, in these systems, it seems possible that the SC state and nonmagnetic state border on each other. Recently, Seo and Fukuyama reported a theoretical approach for the ground state of the π-electron system of λ-$(BETS)_2GaBr_xCl_{4-x}$.[32] They pointed out that this two-dimensional conducting system is located near the boundary of an antiferromagnetic phase and a spin-gap phase. According to their theory, the spin-gap state is weakened by the side-by-side interaction and the two-dimensional AF ground state will appear. It is also indicated that in the system located in the AF phase near the transition point to the "spin-liquid" state whose spin gap decreases with increasing two-dimensional interaction, the susceptibility behaves as $\chi(T) = \chi_0 + aT^2$, not vanishing at 0 K.[33]

Let us imagine here a simple situation where one electron (in this case carrier is hole) is localized on every BETS dimer (see Figure 10c); then there are two holes in the unit cell. As concerns the one-dimensional direction of the BETS stacking, the AF interaction can be expected between these holes: $J_B \propto s_B^2$ and $J_C \propto s_C^2$ (see Figure 2b and Table 4). The enhanced difference between J_B and J_C in the higher x region will produce the energy gap in the localized π spin system, and the interaction J_B is almost independent of x at $x > 0.7$. This suggests that the possible energy gap will be reduced with decreasing x (increasing s_C). At room temperature, holes can manage to move despite its strong correlation when x is small. With increasing x (decreasing s_C), the correlation is enhanced. Because there are two holes in a unit cell, a spin-singlet state will be more stable for the localized holes' ground state, which causes the increasing resistivity and decreasing magnetic susceptibility. With lowering temperature, s_C increases and the correlation is weakened. When x is small ($x < 0.7$), the metallic state emerges below 30−100 K. On the contrary, when x is over 0.8, the correlation is not weakened enough to cause a metallic state even at low temperature and then the insulating ground state is realized (see Figures 3 and 8). Below 10 K, the competition between the SC state and insulating state will appear when x is ∼0.7.

Actually, it is impossible to neglect the interactions J_p-J_t, and these two-dimensional interactions will tend to suppress the spin-singlet state. Thus the AF spin excitation would be expected in the lower x systems. This situation will be consistent with that predicted by Seo and Fukuyama.[32] The erratic susceptibility behavior observed in λ-$(BETS)_2GaBr_{0.7}Cl_{3.3}$ around 20 K would be ascribed to the AF spin fluctuation. It seems that the residue of the susceptibility near 0 K ($x > 1.0$) also indicates the λ system located in the border region of the AF insulator phase and nonmagnetic insulator.

Conclusion

λ-$(BETS)_2GaBr_xCl_{4-x}$ ($0 < x < 2$) gives a series of unique organic conductors whose electronic properties can be continuously changed by controlling the Br content (x). At ambient pressure, the system shows a systematic x-dependence of the resistivity behavior: (1) At $x < 0.55$, the electrical properties change as semiconductor → metal → superconductor; (2) at $0.55 < x < 0.75$, semiconductor → metal → insulator → superconductor; (3) at $x > 0.75$, semiconductor → insulator. The SC state of λ-$(BETS)_2GaCl_4$ is in almost a perfect Meissner state. The magnetic susceptibility measurements of λ-$(BETS)_2GaBr_xCl_{4-x}$ ($x = 1.0, 1.3$) indicate the insulating ground state not to be AF but probably nonmagnetic. The x-dependence of the intermolecular overlap integrals of the HOMOs of BETS molecules indicates that the magnitude of the energy gap of the spin system tends to be diminished for the lower x system where the SC transition takes place. There remains the possibility that the strong suppression of the susceptibility observed at 20−50 K in λ-$(BETS)_2GaBr_xCl_{4-x}$ ($x = 0.7$) is connected with the AF spin fluctuation in the highly correlated metallic state.[34]

Acknowledgment. The authors thank Dr. F. Sakai (Institute for Solid State Physics) for the EPMA measurements, Professor H. Fukuyama and Dr. H. Seo (School of Science, The University of Tokyo) for the theoretical discussion, and Professor K. Kanoda, Dr. K. Miyagawa, Dr. H. Taniguchi (Department of Applied Physics, The University of Tokyo), and Dr. Y. Nakazawa (Institute for Molecular Science) for valuable information and discussions. This work was supported by a Grant-in-Aid for Scientific Research (B) (2) "The phase diagram of new organic superconductor BETS salts with a mixed halogeno gallium anion" (08454217) from the Ministry of Education, Science, Sports and Culture, Japan.

Supporting Information Available: Since all compounds in this paper are isomorphous and the compounds of $x = 0.00$ and 1.50 have already registered to CCDC, the supplementary structure data of only $x = 2.00$ at 293 K and $x = 0.30$, 1.30 at 7 K are available: tables of crystal data, experimental details, atomic parameters, atomic coordinates, bond lengths and angles and ORTEPs for λ-$(BETS)_2GaBr_xCl_{4-x}$, $x = 2.00$ (48 pages, print/PDF). See any current masthead page for ordering information and Web access instructions.

JA9827806

(32) Seo, H.; Fukuyama, H. *J. Phys. Soc. Jpn.* **1997**, *66*, 3352−3355.
(33) Troyer, M.; Zhitomirsky, M. E.; Ueda, K. *Phys. Rev.* **1997**, *B55*, R6117−6120.

(34) After submission of this paper, the broadening of the line width of the signal in ^1H NMR experiments (K. Kanoda; et al., private communications) was observed in λ-$BETS_2GaBr_{1.3}Cl_{2.7}$ around 8 K. Owing to the Curie impurities, the susceptibility below 10 K could not be determined accurately. Nevertheless it may be said that the anisotropy of the susceptibility below 8 K seems to be very small compared with the usual antiferromagnetic systems even if it really exists.